


 Cite this: *RSC Adv.*, 2024, **14**, 27074

# Study of mixed matrix membranes with *in situ* synthesized zeolite imidazolate frameworks (ZIF-8, ZIF-67) in polyethersulfone polymer for CO<sub>2</sub>/CH<sub>4</sub> separation†

 Aditya Jonnalagedda and Bhanu Vardhan Reddy Kuncharam \*

Biogas, produced from anaerobic digestion, is a sustainable and renewable energy source. To upgrade biogas to Bio-CNG, CO<sub>2</sub> must be removed from the raw mixture. Membrane separation is an economical process for the removal of CO<sub>2</sub>, and mixed matrix membranes (MMMs) are being explored for CO<sub>2</sub>/CH<sub>4</sub> separation. MMMs are fabricated using techniques such as *in situ* techniques to overcome research gaps, such as in filler agglomeration and filler–polymer interfaces. In this work, MMMs were fabricated using the *in situ* growth of ZIF-8 and ZIF-67 in polyethersulfone (PES) and compared with traditional filler dispersion of ZIF-8 and ZIF-67. The fabricated MMMs were characterized and tested for gas permeation using a model biogas. Fourier-transform infrared (FTIR) spectroscopy and Field Emission Scanning Electron Microscopy (FESEM) analysis were conducted to confirm *in situ* synthesis of ZIF-8 and ZIF-67. CO<sub>2</sub> permeability of *in situ* ZIF-8 and ZIF-67-based MMMs have enhanced to 84.5 Barrer and 78.8 Barrer, respectively, compared to pure PES membrane, which is around 25 Barrer. Similarly, ZIF-8 and ZIF-67-based traditional MMMs have shown an increase in the CO<sub>2</sub> permeability of 75.6 Barrer and 68 Barrer, respectively. Additionally, the selectivity for CO<sub>2</sub>/CH<sub>4</sub> separation increased for some of the prepared MMMs, demonstrating the effectiveness of the *in situ* fabrication method.

 Received 16th June 2024  
 Accepted 20th August 2024

 DOI: 10.1039/d4ra04400b  
[rsc.li/rsc-advances](http://rsc.li/rsc-advances)

## 1 Introduction

The increase in energy consumption (especially from fossil fuels) in the world has resulted in higher than usual greenhouse gas (GHG) emissions and various unfavorable effects, such as melting polar glaciers, climate change, loss of biodiversity, *etc.*<sup>1</sup> Steps are needed to remedy the impact of GHG emissions, such as carbon dioxide capture and switching to renewable energy sources (such as biogas).<sup>2</sup> Carbon dioxide is separated using chemical and environmental engineering techniques such as adsorption, absorption, cryogenic separation, bio-separation, and gas separation membranes.<sup>3</sup> The membrane separation is one of the cost-effective methods for the removal of carbon dioxide from gas mixtures like biogas (CO<sub>2</sub>/CH<sub>4</sub>),<sup>4</sup> flue gas (CO<sub>2</sub>/N<sub>2</sub>), syngas (CO<sub>2</sub>/H<sub>2</sub>), and also for gas mixtures such as oxygen from the air (O<sub>2</sub>/N<sub>2</sub>),<sup>5</sup> petroleum-based gas separations (C<sub>3</sub>H<sub>8</sub>/C<sub>3</sub>H<sub>8</sub>).<sup>6</sup>

Commercial polymers such as cellulose acetate (CA), polysulfone (PSF), polyether sulfone (PES, UDEL), polyimide (Matrimid 5218), polyether (block imide) (Pebax MH1657) have

been used in gas separation applications. The polymeric membranes employ a solution diffusion mechanism for gas separation,<sup>7</sup> which is efficient and low cost but has a trade-off relation between selectivity and permeability, quantified by Robeson *et al.* 1991 and 2008.<sup>8,9</sup> These challenges can be overcome by using mixed matrix membranes (MMMs); MMMs are fabricated by dispersing inorganic fillers such as metal–organic frameworks (MOF) (ZIFs, UiO-66, MILs), silica, zeolites (H-zeolite, Y-zeolite, ZSM-5), *etc.* in many commercial polymers or synthesized polymers (PIM-1). However, agglomeration at higher filler loading, poor polymer–filler compatibility, polymer rigidification, and the formation of micro-voids and nano-defects may affect the separation performance of the mixed matrix membranes.

Several methods are suggested to overcome these difficulties, such as functionalization of filler, dual filler approach, and *in situ* synthesis.<sup>10</sup> Briefly, the filler particles are added to the polymer solution to fabricate traditional (*ex situ*) MMMs and *in situ* MMMs are fabricated including various types such as *in situ* polymerization – where the growth/coating of filler (mostly MOF) on the surface of the polymer support by using various techniques such as contra diffusion, layer-by-layer coating, *etc.*,<sup>11</sup> *in situ* synthesis of MOF in the polymer and *in situ* synthesis of polymer in MOF solution. All these *in situ* techniques help enhance MMM's properties such as better polymer–

Department of Chemical Engineering, Birla Institute of Technology & Science, Pilani, Pilani Campus, Rajasthan, 333031, India. E-mail: [bhanu.vardhan@pilani.bits-pilani.ac.in](mailto:bhanu.vardhan@pilani.bits-pilani.ac.in); Tel: +91-1596255839

† Electronic supplementary information (ESI) available. See DOI: <https://doi.org/10.1039/d4ra04400b>



MOF interaction, reduce agglomeration and avoid multistep membrane fabrication procedures. For the preparation of MOF in the polymer solution, the synthesis procedure must be simple and have as few steps as possible. So, ZIF-based fillers, especially ZIF-8 and ZIF-67 MOFs are used in various types of applications in catalysis,<sup>12,13</sup> sensors,<sup>14</sup> and pharmaceuticals<sup>15</sup> due to their tuneable pore size, high surface area, and highly chemically and thermally stable. ZIF-8 and ZIF-67 have been widely used in many separation-based studies, such as water remediation and gas adsorption, and as fillers in mixed matrix membranes for gas separation because of their stability in the polymer chain and molecular sieving capability.<sup>16</sup>

Many *in situ*-based studies in gas separation membranes are studied to enhance CO<sub>2</sub> separation; in Jia *et al.* 2023,<sup>17</sup> a study of *in situ* interfacial crosslinking *via in situ* polymerization was done by dispersing NH<sub>2</sub>-MIL-53 MOF in the polyamic acid (PAA) and then polymerized into polyimide (PI) by thermal imidization forming amine (–NH<sub>2</sub>) and hydrogen (H<sub>2</sub>) bonds improving the H<sub>2</sub>/CO<sub>2</sub> separation performance by 400% and CO<sub>2</sub> permeability from 3 to 20 Barrer, this study shows the strong interaction of NH<sub>2</sub>-MIL-53 and PI in the membrane using characterization, gas permeation, and also the effect of the –NH<sub>2</sub> group on H<sub>2</sub>/CO<sub>2</sub> selectivity. A similar study was done by coating PAA on the top of porous  $\alpha$ -alumina supports and immersing in the metal solution (zinc) and linker (benzimidazole) solution alternatively to form ZIF-7 on the top of the PAA layer and then thermally imidized, CO<sub>2</sub> permeability has dropped (from 433 to 74 Barrer) but improved CO<sub>2</sub>/CH<sub>4</sub> selectivity from 29 to 36,<sup>18</sup> and a similar study was conducted previously by the same corresponding authors<sup>19</sup> group for propylene-selective membranes using polymer-modification-enabled *in situ* metal-organic framework formation (PMMOF), *in situ* synthesis of ZIF-8 was done on the porous support coated with 4,4-(hexafluoroisopropylidene)di-phthalic anhydride 2,4,6-trimethyl-1,3-phenylenediamine polymer, both studies show that the ZIF synthesis using PMMOF method has enlarged the free volume of polymer which helped ZIF growth *via* the absorption of excess Zn-ion sources. In another *in situ* study, *in situ* grafting of polyethylene amine on ZIF-8 was done and dispersed in poly(vinyl amine) (PVAm) and coated of modified polysulfone (PSF) substrate, and selectivity of CO<sub>2</sub>/CH<sub>4</sub> improved from 20 to 50. This increase is attributed to the stable porous structure of PEI-g-ZIF-8 particles inside the polymer matrix and showed good compatibility with PVAm. Also, CO<sub>2</sub> permeance improved around 3800 GPU.<sup>20</sup> In a study done by Xio li *et al.* for CO<sub>2</sub>/N<sub>2</sub> separation, where MMMs were fabricated using ZIF-8 *in situ* inserted by functionalized multiwall carbon nanotubes (MWCNTs) (*i.e.*, ZIF-8 is synthesized in the solvent with MWCNTs dispersed) and Pebax polymer for improving the membrane's free volume and to provide CO<sub>2</sub> channelling through ZIF-8 particles inside the smooth surface of MWCNTs. The functional groups of MWCNTs have given dispersion and without agglomerates of filler particles in MMMs. This has improved CO<sub>2</sub> permeability to 186.3 Barrer from 80 Barrer, selectivity CO<sub>2</sub>/N<sub>2</sub> from 30 to 61.3 and has surpassed Robeson upper bound.<sup>21</sup> *In situ* synthesis of UiO-66 was done in polyimide polymer (Matrimid 5218), and MMMs were fabricated

using the drop-casting method on Petri dishes, where ideal CO<sub>2</sub>/N<sub>2</sub> selectivity and CO<sub>2</sub> permeability of 11 wt% *in situ* UiO-66/PI was found at 36 and 24 Barrer, respectively, improved from 34 and 19 Barrer for 11 wt% UiO-66/PI.<sup>22</sup> This paper provides good insights into growing of UiO-based MOF in PI polymer using a novel approach. To enhance the filler/polymer interfacial compatibility and decrease the agglomerates of ZIF-8 MOFs, an *in situ* technique was used to synthesize ZIF-8 particles in the Pebax-2533 (by one-pot synthesis), and MMMs were cast on fabricated PES support layer for CO<sub>2</sub>/CH<sub>4</sub> separation studies, where CO<sub>2</sub> permeability and CO<sub>2</sub>/CH<sub>4</sub> selectivity was enhanced by 155% and 144% respectively at 8 bar feed pressure overcoming Robeson lower bound.<sup>23</sup>

The literature survey for some of the above *in situ* studies shows the gas separation potential of ZIF-based MOFs and their compatibility with various polymers, which leads to various explorations for its *in situ* fabrication to enhance its properties for CO<sub>2</sub>/CH<sub>4</sub> separation. Most of the available investigations have focused on the fabrication of *in situ* MMMs with PI and Pebax polymers and studies for gas separation mostly with pure gases at high pressures. However, *in situ* synthesis of MOF in PES polymer and fabrication of its MMMs for CO<sub>2</sub> separation has not been demonstrated yet and studied for CO<sub>2</sub>/CH<sub>4</sub> separation with mixed gas at lower pressures based on our literature survey. To address this research gap, in the current study, in a novel approach, MMMs were prepared using *in situ* growth of ZIF-8 and ZIF-67 nanoparticles in PES polymer and also by traditional route, *i.e.*, dispersion of ZIF-8, ZIF-67 nanofillers in PES. CO<sub>2</sub>/CH<sub>4</sub> separation studies were done by testing gas permeation with model biogas (60 : 40–CH<sub>4</sub> : CO<sub>2</sub> in vol%) as a feed mixture at pressure differences of 0.5–1.5 bar. Performance analysis of MMMs was done by comparing gas permeation results of *in situ* and non-*in situ* MMMs.

## 2 Experimental

### 2.1. Materials

Zinc nitrate hexahydrate (99%, Zn(NO<sub>3</sub>)<sub>2</sub>·6H<sub>2</sub>O), 2-methylimidazole (99%, 2-MeIM), and cobalt nitrate hexahydrate (Co(NO<sub>3</sub>)<sub>2</sub>·6H<sub>2</sub>O) was purchased from Merck Life Science Private Ltd, India. Polyethersulfone (PES) was purchased from Solvay Chemicals, India. Solvents such as methanol (CH<sub>3</sub>OH) and dimethyl formamide (DMF) were obtained from Merck Life Science Private Ltd, India, and Rankem Chemicals, India, respectively. Mixed gas (CO<sub>2</sub>/CH<sub>4</sub>) used for the gas permeation test was procured from Ankur Speciality Gases and Technologies Private Ltd, Jaipur, India.

### 2.2. Synthesis of ZIF-8 and ZIF-67

The synthesis of ZIF-8 filler was adapted using literature<sup>24</sup> where 0.68 g of zinc nitrate hexahydrate and 1.5 g of 2-methylimidazole were mixed in 50 ml of methanol separately. After the solids had been dissolved, the two solutions were combined and stirred overnight until the reaction mixture to the opaque solution. The opaque solution mixture was centrifuged at 7000 rpm for 5 minutes and washed with methanol. The



resulting wet solids were dried in an air oven at 70 °C to eliminate any remaining methanol; the air-dried solids were then dried for an additional night at 100 °C.

Synthesis of ZIF-67 was derived from the literature,<sup>25</sup> where 0.5 g of cobalt nitrate hexahydrate was dissolved in the 25 ml of methanol (reddish brown solution) and 1 g of 2-methylimidazole was dissolved in 25 ml methanol (transparent solution). The two mixtures were mixed into a conical flask and stirred overnight (the solution immediately turned purple). The stirred mixture is then centrifuged and washed with methanol using the same process as previously mentioned to synthesize ZIF-67.

### 2.3. Fabrication of pure PES, ZIF-8, ZIF-67/PES MMMs

Pure PES membrane was prepared by dissolving 3 g of PES polymer powder in 15 ml of DMF solvent using the priming method at 50 °C. After completely dissolving the polymer, the solution was stirred for an additional 5 hours to avoid polymer lumps. The polymer solution was degassed in a vacuum chamber for around 1 hour to eliminate air bubbles formed due to stirring. The polymer dope solution was cast on a flat Petri dish and placed in a vacuum oven at 60 °C for two days for solvent evaporation, draining the solvent in between to form a dense PES membrane, which was peeled off the Petri dish.

ZIF-8 and ZIF-67-based mixed matrix membranes (MMMs) were synthesized by suspending predetermined amount of MOF-filler in 15 ml of DMF (for 1, 2, 4, 5, 10, 15, and 20 wt%) using eqn (1). The MOF solution was sonicated for 1 hour, and then 3 g of polymer was added to the MOF solution and stirred overnight. The MOF-polymer mixture was sonicated for 3 hours and degassed for 1 hour; the same membrane casting and drying procedure was followed for pure PES membrane. The fabrication technique of MMMs is shown in Fig. 1a

$$\text{MOF\% loading} =$$

$$\frac{\text{Weight of the ZIF-8 or ZIF-67}}{\text{Weight of the ZIF-8 or ZIF-67} + \text{Weight of the polymer}} \quad (1)$$

### 2.4. Synthesis *in situ* ZIF-8 and ZIF-67 in PES polymer solution and MMMs fabrication

A novel *in situ* synthesis method for ZIF-8 and ZIF-67 was developed with various optimizations, in which a predetermined amount of metal precursor (zinc nitrate salt for ZIF-8 and cobalt nitrate salt for ZIF-67) and linker (2-MeIM) separately in 2.5 ml DMF solution based on yields obtained for synthesis of ZIF-8 (16.6%) and ZIF-67 (15.62%).<sup>23</sup> In this method, 3 g of PES polymer was pre-dried at 50 °C and then dissolved in 10 ml of DMF using a priming technique. After stirring for 1 hour, both solutions (metal and linker) were mixed together in a polymer solution and stirred for 1 hour to form MOF particles, followed by overnight stirring for the uniform mixture. A similar procedure was used as the PES membrane was cast with a dope solution, and the same drying temperature was used, but the *in situ* membrane drying time was three days. Further, MMMs were dried overnight in an air oven at 50 °C to

remove additional solvent trapped in pores. The fabrication of MMMs using *in situ* technique is shown in Fig. 1b.

### 2.5. Characterization of ZIF-8, ZIF-67 and characterization of all membranes

X-ray diffraction (XRD) characterization was done for ZIF-8 and ZIF-67 MOFs using a tabletop Rigaku Miniflex X-ray diffractometer using Cu-K $\alpha$  radiation ( $\lambda = 1.54 \text{ \AA}$ ) with 30 kV and 15 mA to analyse the crystal structure, XRD spectra was collected in range 5–40° at a scanning rate of 2° per minute. Fourier Transform Infrared spectroscopy (FTIR) analysis was done for ZIF-8, ZIF-67, and all prepared MMMs to confirm the chemical bonding present in the MOFs and MMMs using a PerkinElmer Frontier Spectrometer where the sample is prepared using a KBr press (Model M-15) and data was acquired in the 400–4000  $\text{cm}^{-1}$  IR zone. The glass transition temperature ( $T_g$ ) for all membranes was obtained using a differential scanning calorimeter (DSC) (PerkinElmer DSC 400), in the temperature range 30–270 °C with nitrogen at 20  $\text{ml min}^{-1}$  with heating and cooling rate of 10 °C  $\text{min}^{-1}$ . The morphology of the membranes was characterized using Field Emission Scanning Electron Microscope (FESEM, FEI-ApreoLoVac model), where all the membranes were placed on stubs with carbon tape and coated with gold in a vacuum chamber for 30 seconds; the coated grids were placed at a 45° angle to electron gun to obtain the cross-sectional morphology of membranes.

### 2.6. Gas permeation tests

A detailed schematic of the gas permeation setup is reported in our previous study.<sup>26</sup> The fabricated membranes were placed between two rubber gaskets where gas permeation experiments were carried out by sending feed of mixed gas with a composition of  $\text{CO}_2 : \text{CH}_4 = 40 : 60$  by regulating a flow of 13  $\text{cc min}^{-1}$  using mass flow controller (MFC) and pressure difference of 0.5, 1 and 1.5 bar between permeate and feed chamber were maintained using a Back Pressure Regulator (Swagelok-BPR). Nitrogen is used as a sweep gas in the permeate chamber. Permeate and retentate streams are connected to gas chromatography with a TCD detector (Shimadzu 2014) to analyse their concentrations and also to permeate side to the bubble flow meter to measure the permeate flow, which is used to measure membranes gas permeability and selectivity using eqn (2) and (3), respectively.<sup>26</sup>

$$P = \frac{Q \times l}{A \times \Delta p} \quad (2)$$

where  $Q$  is the permeate flow rate ( $\text{cm}^3 \text{ s}^{-1}$ ),  $l$  is the membrane thickness (in cm),  $A$  is the membrane area (in  $\text{cm}^2$ ),  $\Delta p$  is the partial pressure difference of the gas species on the permeate and retentate side (in cm Hg).

Selectivity ( $\alpha_{\text{CO}_2/\text{CH}_4}$ , no units) is the ratio of permeabilities of  $\text{CO}_2$  and  $\text{CH}_4$ .

$$\alpha_{\text{CO}_2/\text{CH}_4} = \frac{P_{\text{CO}_2}}{P_{\text{CH}_4}} \quad (3)$$



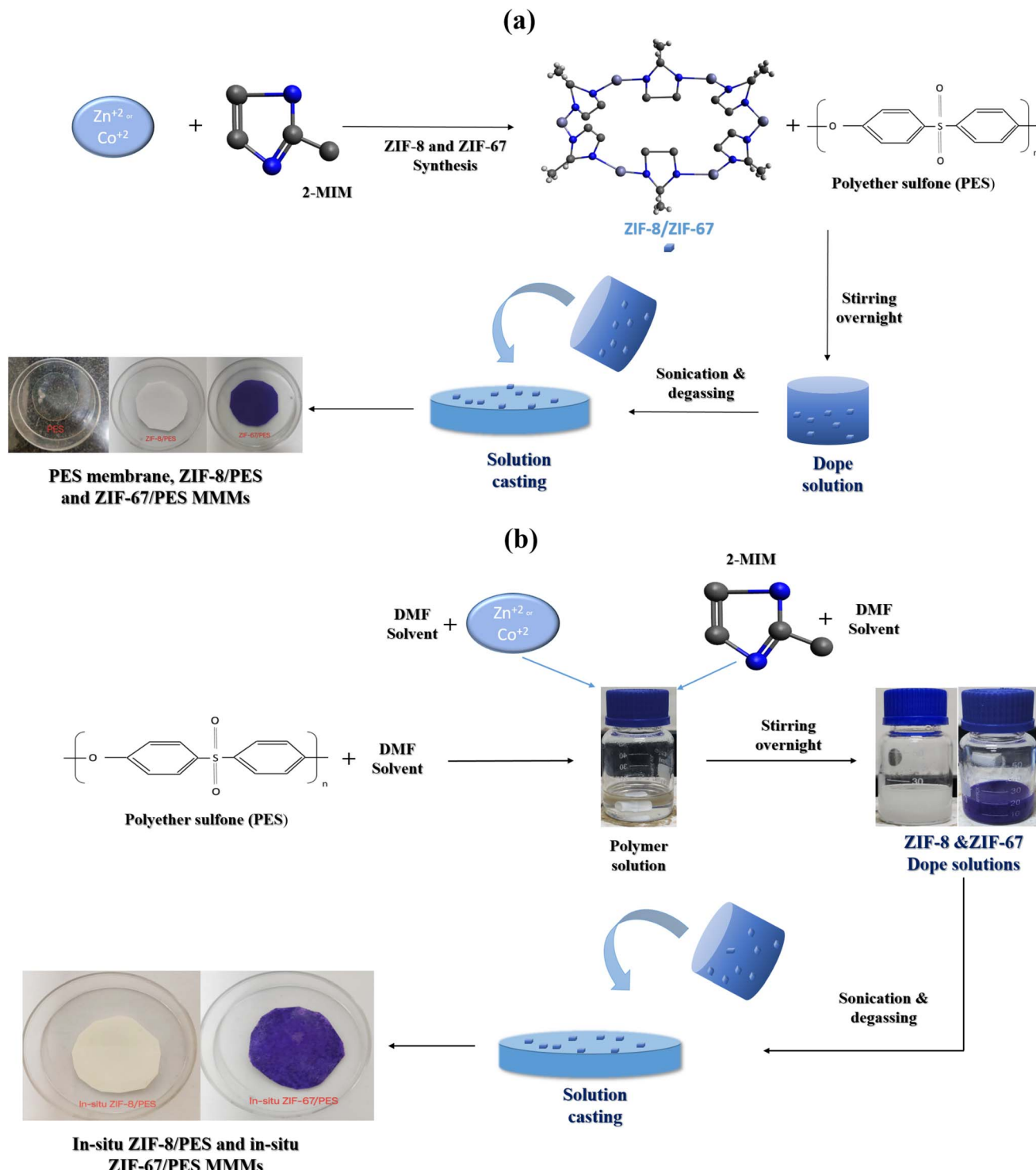


Fig. 1 Schematic for preparation of MMMs via (a) traditional method and (b) *in situ* method.

### 3 Results and discussion

#### 3.1. Characterization of MOFs and membranes

**XRD of ZIF-8, ZIF-67, and MMMs.** Fig. 2a shows the XRD of ZIF-8 and ZIF-67, the sharp peaks of 2 theta values representing the miller indices (1 1 0), (2 0 0), (2 1 1), (2 2 0) and (2 2 2) form

which we can confirm the crystalline structure of both MOFs (ZIF-8, ZIF-67) from the literature<sup>27</sup> and sharp peaks indicating the purity of the material. The additional peaks formed correspond to (1 1 4), (2 3 3), (0 4 4), (3 4 4), (2 4 4), and (2 3 5) (as shown in Fig. 2a) are good agreement with previous studies.<sup>28</sup> Fig. 2b shows XRD patterns of PES, membranes, ZIF-8, ZIF-67, and *in situ* ZIF-8, ZIF-67 MMMs. Pure PES membrane shows



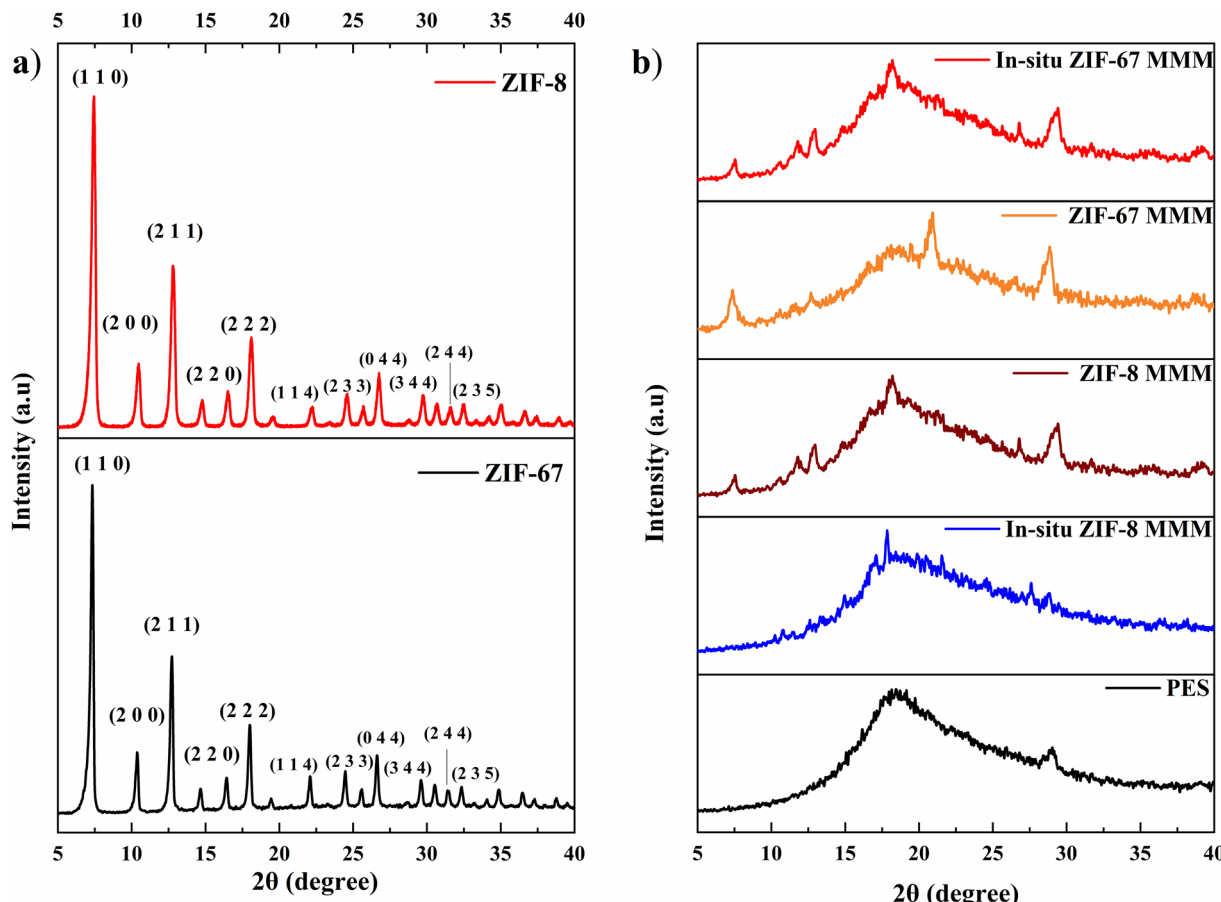


Fig. 2 XRD of (a) MOFs and (b) membranes.

a broad peak at  $18.52^\circ$ , indicating its amorphous nature.<sup>29</sup> The sharp peaks are observed within the broad peaks of PES, which indicates the incorporation of filler ZIF-8 and ZIF-67 in PES and confirms the successful *in situ* synthesis of ZIF-8 and ZIF-67 in PES polymer. MMMs crystallinity was observed by intersegmental distance (or *d*-spacing), which is calculated using Bragg's formula.<sup>30</sup> The *d*-spacing of pure PES membrane was found to be 0.47 nm, which represents polymer chains that are densely packed within the polymeric membrane. For membrane samples of ZIF-8 MMM, ZIF-67 MMM, *in situ* ZIF-8 MMM, and ZIF-67 MMM, the *d*-spacing values are 0.49 nm, 0.44 nm, 0.51 nm, and 0.49 nm respectively, this change in the *d*-spacing of membranes show added MOF fillers are settled in polymer chains and crystallinity was introduced into amorphous polymeric membranes.

**FTIR of MOFs and membranes.** FTIR spectra of ZIF-8 and ZIF-67 were shown in Fig. 3a, in which both MOFs show characteristic peaks around  $3200\text{ cm}^{-1}$  representing the N–H stretch and entire peaks around  $2900\text{ cm}^{-1}$  indicating the imidazole unit. The peaks around  $1550\text{ cm}^{-1}$  and  $1260\text{ cm}^{-1}$  are due to C–N stretch and N–H bend, respectively, and peaks in between  $600\text{ cm}^{-1}$  and  $1100\text{ cm}^{-1}$  are due to alkene and alkane stretching inside the aromatic ring of 2-methylimidazole. The sharp peaks at  $423\text{ cm}^{-1}$  (for ZIF-8) and  $425\text{ cm}^{-1}$  (for ZIF-67) correspond to Zn–N(Im) and Co–N(Im), respectively, *i.e.*, the

peaks show the bond between metal (Zn or Co) to nitrogen present in the organic linker (2-MeIM).<sup>31</sup>

Fig. 3b shows the FTIR spectra of pure PES membranes, 1 wt% and 20 wt% of ZIF-8 and ZIF-67/PES MMMs and 1 wt% and 5 wt% of *in situ* ZIF-8 and ZIF-67/PES MMMs. In the FTIR plot, we can see that all characteristic peaks of PES polymer, *i.e.*, C–N stretch (around  $3000\text{ cm}^{-1}$ ), benzene ring stretch (at about  $1510\text{ cm}^{-1}$ ), and  $-\text{SO}_2-$  ( $1095\text{ cm}^{-1}$ )<sup>32</sup> are present in all membranes after introducing the fillers. No additional peaks or peak shifting were observed except for bonds around  $420\text{--}425\text{ cm}^{-1}$  (present only in MMMs), which are attributed to metal linker Zn–N(Im)/Co–N(Im) bonding, as mentioned in the above section. The FTIR spectra of MMMs also show no additional peaks, indicating the addition of filler has not hampered the structural chain of the polymer and filler particles have settled within the free volume of the polymer, which corresponds to the XRD results where MMMs peaks still represent the amorphous nature of the polymer.

**DSC of membranes.** The glass transition temperature ( $T_g$ ) of membranes obtained from DSC data is shown in Table 1. Pure PES membrane  $T_g$  was found to be around  $220\text{ }^\circ\text{C}$ .<sup>33</sup> It is observed that  $T_g$  values of all MMMs have increased with filler loading, *i.e.*, ZIF-8/PES MMMs from  $223\text{ }^\circ\text{C}$  to  $230\text{ }^\circ\text{C}$ , similarly for ZIF-67/PES MMMs  $224\text{ }^\circ\text{C}$  to  $233\text{ }^\circ\text{C}$  from 1 wt% to 20 wt% respectively. The  $T_g$  values of *in situ* MMMs for both ZIF-8 and



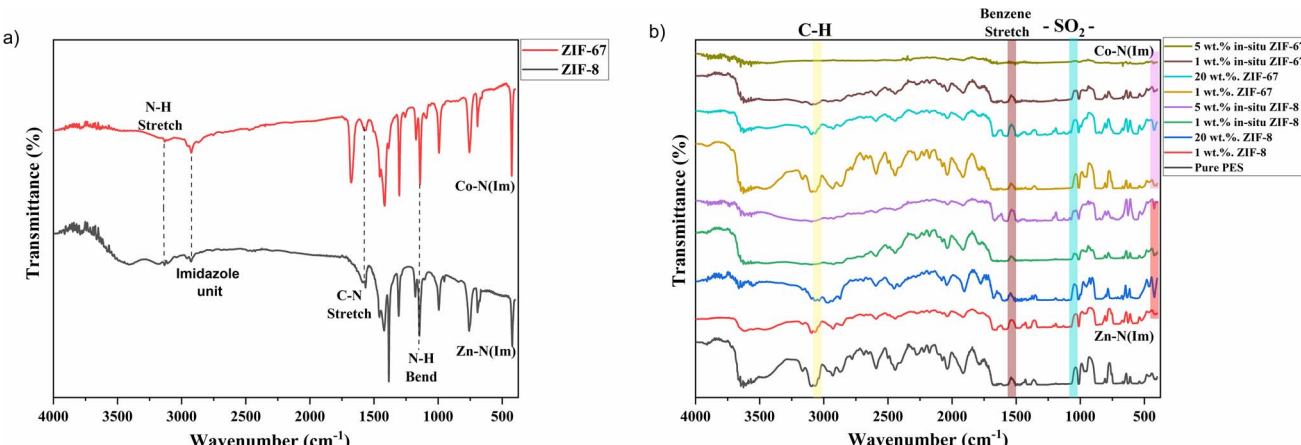


Fig. 3 FTIR of (a) ZIF-8 and ZIF-67, (b) pure PES and MMMs.

Table 1 DSC data ( $T_g$ ) of membranes

Membrane	$T_g$ (°C)
Pure PES	$220.5 \pm 0.6$
1 wt% ZIF-8 PES	$223.1 \pm 0.7$
20 wt% ZIF-8 PES	$230.9 \pm 0.2$
1 wt% <i>in situ</i> ZIF-8 PES	$225.2 \pm 0.9$
5 wt% <i>in situ</i> ZIF-8 PES	$227.4 \pm 0.4$
1 wt% ZIF-67 PES	$223.9 \pm 0.3$
20 wt% ZIF-67 PES	$233.8 \pm 0.5$
1 wt% <i>in situ</i> ZIF-67 PES	$227.6 \pm 0.3$
5 wt% <i>in situ</i> ZIF-67 PES	$229.4 \pm 0.4$

ZIF-67 are slightly higher than traditional MMMs (1 wt% *in situ* ZIF-8/PES – 225 °C, 1 wt% *in situ* ZIF-67/PES – 227 °C). This increase in  $T_g$  values for *in situ* MMMs can be interpreted as higher polymer rigidification compared to traditional MMMs. The formation of the rigidified polymer at the MOF-polymer interface and good dispersion of the inorganic phase is shown by the increase in  $T_g$ .<sup>34</sup> Also, the higher polymer rigidification in membranes indicates the increase of crystallinity of PES, which is in good agreement with XRD results.

**FESEM.** Cross-section FESEM images of pure PES and some mixed matrix membranes (MMMs) are shown in Fig. 4 and S1.† Fig. S1† shows the pure PES membrane cross-section images with no pinholes, cracks, or voids, and the membranes are smooth and dense. Fig. 4a and b shows FESEM images of 1 wt% ZIF-8/PES and 20 wt% ZIF-8/PES MMMs respectively, where we can see the particle size of ZIF-8 was 55.47 nm and 65.2 nm, respectively, in the PES matrix, and the increase in particle size may be due to agglomeration of MOF particles. In Fig. 4e and f, we can see that the particle size of ZIF-67 MOF in higher (1 wt%) and lower (20 wt%) filler loading has remained almost the same (50.98, 50.39 nm) irrespective of the agglomeration, which can be seen in Fig. 4f. The particle size of ZIF-8 in Fig. 4c and d *in situ* ZIF-8 MMMs (1 wt%–75.72 nm and 5 wt%–105.77 nm) has increased compared to traditional MMMs (1 wt%–55.47 nm), this increment may be due to the synthesis of ZIF-8 PES polymer. ZIF-67 particle size in *in situ* MMMs from Fig. 4g and h of

1 wt% ZIF-67/PES and 5 wt% ZIF-67/PES respectively, 1 wt% ZIF-67 MMM particle size was 95.33 nm, which has increased similarly due to the synthesis of MOF in polymer and for 5 wt% ZIF-67 MMM particle size has slightly increased (to 62 nm), but we can see the formation of voids in the membrane.

We can also observe the growth of ZIF-particles in polymer; in Fig. 4c and d, we can see that the particle growth of *in situ* ZIF-8 has increased compared to ZIF-8 in traditional (*ex situ*) MMMs due to an increase in stirring time, temperature and also change in solvent<sup>35</sup> which led to Sono-crystallization.<sup>36</sup> *In situ* ZIF-67 particles have shown a huge rough growth rate at higher metal concentration<sup>37</sup> which led to the formation of defects in the membrane, as shown in Fig. 5h. Despite the formation of defects in 5 wt% *in situ* ZIF-67 MMM due to the rough growth rate, XRD and FTIR spectra of the membrane show that there is no structural damage within polyethersulfone polymer.

### 3.2. Gas permeation experiments

**Permeation tests of ZIF-8 and ZIF-67 based MMMs (effect of fillers).** Gas permeation experiments were conducted for all prepared membranes (pure PES and ZIF-8/ZIF-67 MMMs) at 0.5 bar pressure difference and presented in Tables 2 and 3. In Table 2, we can see that the permeability of CO<sub>2</sub> is enhanced with an increase in filler (ZIF-8) loading; pure polymer showed CO<sub>2</sub> permeability of 24 Barrer, where we can see upon adding 15 wt% of ZIF-8 permeability has increased to 75 Barrer, which is 212% increase compared to pure polymeric membrane and decreased at 20 wt% ZIF-8 to 47 Barrer (37% decrease compared to 15 wt% ZIF-8). The decrease in permeability might be due to the polymer (PES) rigidification by ZIF-8 MOF at higher filler loading (20 wt%) during membrane preparation, which can be seen in the increment of  $T_g$  values in the Table 1, where membrane/polymer restricts the gas transport.<sup>34</sup> The CO<sub>2</sub>/CH<sub>4</sub> selectivity of ZIF-8 PES MMMs has increased at 15 wt% ZIF-8, which is only a 16% increase (from 12 to 14). The pure polymeric membrane and the rest of all MMM's selectivity were in the range of 12–13 (almost the same as the PES membrane). This decrease in CO<sub>2</sub>/CH<sub>4</sub> selectivity of the MMMs can be due to



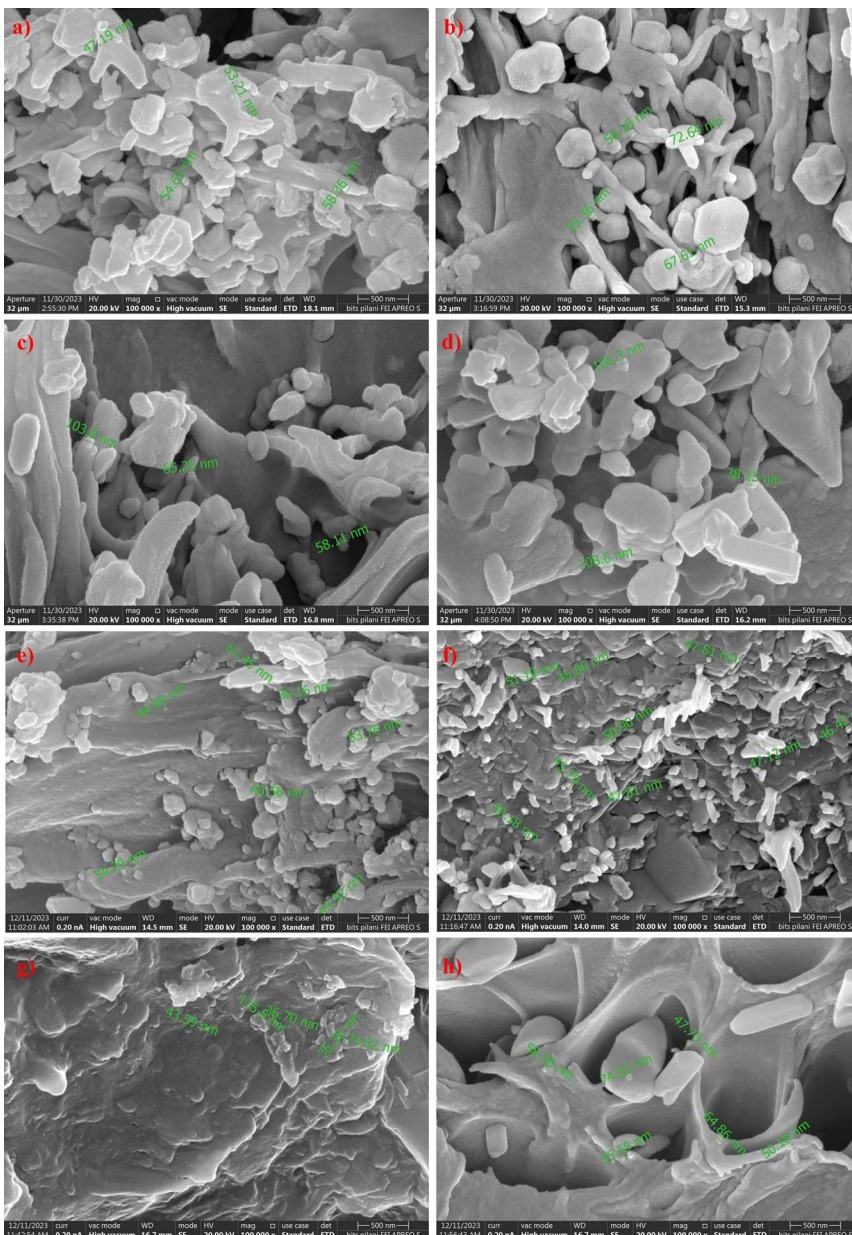


**Fig. 4** FESEM images—cross-section view of (a and b) 1, 20 wt% ZIF-8 MMMs, (c and d) 1, 5 wt% *in situ* ZIF-8 MMMs, (e and f) 1, 20 wt% ZIF-67 MMMs, (g and h) 1, 5 wt% *in situ* ZIF-67 MMMs.

two reasons: (1) agglomeration of ZIF-8 MOF particles, which can be seen in the FESEM image<sup>38</sup> (Fig. 4b) of 20 wt% ZIF-8/PES, where the particle size of ZIF-8 was also increased, and (2) ZIF-8 has a pore aperture size of 3.4 Å, should ideally also increase  $\text{CO}_2/\text{CH}_4$  selectivity (molecular sieving effect because of  $\text{CO}_2$  and  $\text{CH}_4$  molecular diameter of 3.3 and 3.8 Å, respectively). However, because of its limited flexibility and complete frigid saturation, ZIF-8 absorbs relatively close kinetic diameter gases, which lowers the  $\text{CO}_2/\text{CH}_4$  selectivity.<sup>39</sup>

In Table 3, we can see the  $\text{CO}_2$  permeability and  $\text{CO}_2/\text{CH}_4$  selectivity of ZIF-67/PES MMMs where the addition of ZIF-67 filler has initially decreased  $\text{CO}_2$  permeability from 24 Barrer to 22 Barrer (8% decrease) which can happen for lower filler

loading (1 wt%) due to restricted polymer chain mobility.<sup>40</sup> We can see the increment of permeability from 2 wt% ZIF-67 filler loading to 33 Barrer, which is a 37% increase, and also the highest CO<sub>2</sub> permeability of 68 Barrer (183% increase) at 15 wt% MOF loading and a decrease of 21% at 20 wt% ZIF-67, *i.e.*, from 68 to 54 Barrer, which might be due to polymer rigidification (same as ZIF-8 MMMs) where the  $T_g$  value was increased to 234 °C (from 220 °C). CO<sub>2</sub>/CH<sub>4</sub> selectivity of ZIF-67-based MMMs has risen from 12 to 16 (33% increase) at 5 wt% of ZIF-67, which can be attributed to a size-sieving mechanism of ZIF MOF as mentioned above, selectivity of CO<sub>2</sub>/CH<sub>4</sub> at 20 wt% was slightly decreased (of 6%) to 14.7. All other ZIF-67 MMMs selectivity was around 13–14, higher than pure PES membrane – the reason for

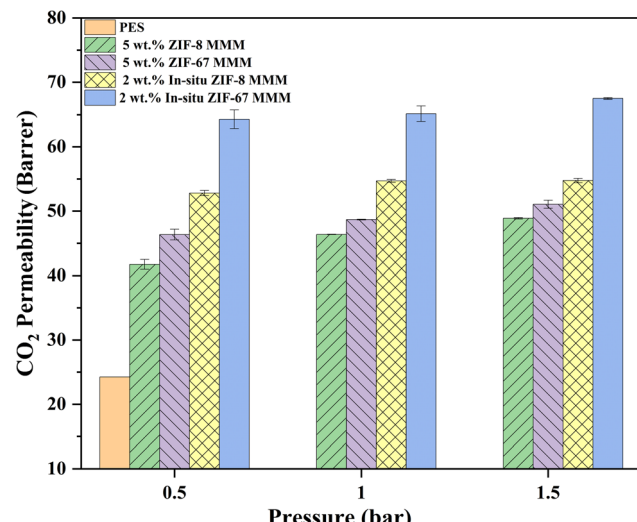


Fig. 5 Variation of CO<sub>2</sub> permeability of MMMs with the increase of pressure.

the drop of selectivity at 20 wt% ZIF-67 MOF may be due to agglomeration, which can be seen in Fig. 4f, and also, we can observe that the particle size of ZIF-67 in 20 wt% ZIF-67/PES MMM has almost remained within the same range as 1 wt% ZIF-67 MMM. This can be why CO<sub>2</sub>/CH<sub>4</sub> selectivity has remained at 15 and not declined below 12.

**Permeation tests of *in situ* ZIF-8 and *in situ* ZIF-67-based MMMs (effect of *in situ* synthesis of fillers).** Tables 4 and 5 show the permeation results of *in situ* ZIF-8 and *in situ* ZIF-67-based MMMs; only 1, 2, 4, 5 wt% of both *in situ* ZIF-8 and ZIF-67 were prepared because the solidification of the polymer during dope preparation at higher filler loading. Even lower filler wt% has good growth in permeability, *i.e.*, for 1 wt% of *in situ* ZIF-8 PES membrane, CO<sub>2</sub> permeability was 33.3 Barrer, which is a 39% increase than pure polymeric membrane. At *in situ* 2 wt% and 4 wt% of ZIF-8 CO<sub>2</sub> permeability was 65 Barrer (170% increase) and 84 Barrer (250% increase), respectively; this may be due to the increase in permeability is because of *in situ* synthesized ZIF-8 with good dispersion (from FESEM images Fig. 4c and 3d) and causes faster diffusion of gases. The permeability of CO<sub>2</sub> was decreased by 27% at 5 wt% *in situ* ZIF-8 MMM from 84 Barrer to 61.2 Barrer. This might be due to an

unreacted linker (2-methylimidazole) in the membrane<sup>41</sup> and an increase in glass transition temperature (T<sub>g</sub>) to 227 °C, which indicates the rigidified polymer at the filler–polymer interface. CO<sub>2</sub>/CH<sub>4</sub> selectivity of *in situ* ZIF-8 MMMs has increased at 4 wt% ZIF-8 *in situ* MMM to 15.21 (27% increase), which is attributed to size sieving ability of ZIF-8, and the rest of the MMMs have not shown improvement in the selectivity of CO<sub>2</sub>/CH<sub>4</sub>, which can be implied to the particle size of ZIF-8, in MMMs as mentioned in FESEM section.

*In situ* ZIF-67-based mixed matrix membranes (MMM) have also shown an increase in the CO<sub>2</sub> permeability (same as *in situ* ZIF-8 PES MMMs) at 1 wt% and 2 wt% *in situ* ZIF-67 MMMs, the permeability of CO<sub>2</sub> was increased from 24 Barrer (pure PES membrane) to 27.8 Barrer and 52.8 Barrer with 16% and 120% increase with respect to PES membrane respectively. The highest permeability of CO<sub>2</sub> of 73.7 Barrer was observed at 4 wt% *in situ* ZIF-67, which is a 207% increase. The CO<sub>2</sub>/CH<sub>4</sub> selectivity also showed an increasing trend for 1, 2, and 4 wt% of *in situ* ZIF-8 is 11.6, 12.76, and 13.47, respectively. This trend might be due to the molecular sieving capacity of ZIF-67 and the adsorption capacity of CO<sub>2</sub> over CH<sub>4</sub>.<sup>42</sup> For 5 wt% *in situ* ZIF-67 MMM has given CO<sub>2</sub> permeability of 79.625 Barrer and CO<sub>2</sub>/CH<sub>4</sub> selectivity of 1.11, correspond to FESEM image Fig. 4h, where the membrane has formed defects due to *in situ* ZIF-67 (as discussed in FESEM section) which has allowed passage for both CO<sub>2</sub> and CH<sub>4</sub> gases.

**Effect of pressure difference on all membranes.** Permeation tests were done at three pressure differences of 0.5, 1, and 1.5 bar, and the values are displayed in Tables 2–5 and effect of pressure on CO<sub>2</sub> permeability in five different membranes was given for better comparison in Fig. 5. We can see CO<sub>2</sub> permeability of all prepared membranes has enhanced and for a few membranes (4 wt% ZIF-8/PES, 15 wt% ZIF-8/PES, and 20 wt% ZIF-8/PES, 4 wt% ZIF-67/PES, 20 wt% ZIF-67/PES, 4 wt% *in situ* ZIF-8/PES, 5 wt% *in situ* ZIF-8/PES, 4 wt% *in situ* ZIF-67/PES and 5 wt% *in situ* ZIF-67/PES) would not withstand higher pressure, this might be due to the lower tensile strength of the membranes at higher filler loading.<sup>43</sup> The highest enhancements were found for 5 wt% ZIF-8/PES from 41.6 Barrer to 48.9 Barrer at 1.5 bar, 10 wt% ZIF-8/PES from 61.9 Barrer to 67.4 Barrer at 1.5 bar, 4 wt% *in situ* ZIF-67/PES from 73.7 Barrer to 78.8 Barrer at 1 bar. CO<sub>2</sub>/CH<sub>4</sub> selectivity was not enhanced to a significant extent, which can be attributed to limitations of

Table 2 ZIF-8/PES MMMs permeation data at 0.5 bar, 1 bar, 1.5 bar

Membrane	CO <sub>2</sub> permeability (Barrer)			CO <sub>2</sub> /CH <sub>4</sub> selectivity		
	0.5 bar	1 bar	1.5 bar	0.5 bar	1 bar	1.5 bar
Pure PES	24.2 ± 0.27	25.7 ± 0.5	25.4 ± 0.63	12.23	14.14	12.61
1 wt% ZIF-8/PES	28.9 ± 0.99	21.9 ± 0.49	31.5 ± 0.68	11.47	13.06	10.38
2 wt% ZIF-8/PES	37.2 ± 1.63	39.9 ± 0.62	39.6 ± 0.54	10.55	10.04	10.76
4 wt% ZIF-8/PES	39.6 ± 0.6	40.3 ± 0.05	—	11.09	11.43	—
5 wt% ZIF-8/PES	41.7 ± 0.76	46.4 ± 0.02	48.9 ± 0.11	11.36	11.51	10.33
10 wt% ZIF-8/PES	61.9 ± 0.31	65.7 ± 0.9	67.4 ± 0.67	11.78	11.32	9.60
15 wt% ZIF-8/PES	75.6 ± 1.59	77.4 ± 0.5	—	13.76	11.96	—
20 wt% ZIF-8/PES	47.7 ± 1.28	—	—	12.28	—	—



Table 3 ZIF-67/PES MMMs permeation data at 0.5 bar, 1 bar, 1.5 bar

Membrane	CO <sub>2</sub> permeability (Barrer)			CO <sub>2</sub> /CH <sub>4</sub> selectivity		
	0.5 bar	1 bar	1.5 bar	0.5 bar	1 bar	1.5 bar
Pure PES	24.2 ± 0.27	25.7 ± 0.5	25.4 ± 0.63	12.23	14.14	12.61
1 wt% ZIF-67/PES	22.0 ± 1.27	23.3 ± 0.02	26.0 ± 0.06	10.02	9.49	13.14
2 wt% ZIF-67/PES	32.9 ± 0.09	33.8 ± 0.34	28.6 ± 0.04	10.46	11.44	11.84
4 wt% ZIF-67/PES	34.8 ± 0.23	—	—	11.50	—	—
5 wt% ZIF-67/PES	46.9 ± 0.83	48.7 ± 0.06	51.1 ± 0.65	15.82	12.87	11.54
10 wt% ZIF-67/PES	54.8 ± 2.17	54.2 ± 0.58	55.1 ± 1.4	13.23	11.74	12.27
15 wt% ZIF-67/PES	68.0 ± 1.88	70.5 ± 0.26	65.4 ± 0.63	14.58	13.51	13.39
20 wt% ZIF-67/PES	54.4 ± 0.88	—	—	14.58	—	—

material properties as mentioned in the above section, and the only exception to this 4 wt% *in situ* ZIF-67/PES MMM has shown improvement of selectivity from 13.47 to 16.39.

**Comparison of ZIF-8 and ZIF-67-based MMMs.** In Fig. S2,† we can see the comparison of CO<sub>2</sub> permeability and CO<sub>2</sub>/CH<sub>4</sub> selectivity of ZIF-8 of ZIF-8/PES and ZIF-67/PES-based MMMs in bar graphs. Fig. S2† clearly shows that ZIF-8/PES MMMs show higher enhancement in CO<sub>2</sub> permeability than ZIF-67/PES MMM of 10 and 15 wt% filler loading for 10 wt% MMMs CO<sub>2</sub> permeability values are 61.9 Barrer (for ZIF-8) and 54.8 Barrer (for ZIF-67) which is 11% higher and for 15 wt% ZIF-8 was 75.6 Barrer and for ZIF-67 was 54.8 Barrer which is 10% higher. At 5 wt% and 20 wt% MMMs of ZIF-67 showed slightly more CO<sub>2</sub> permeability than ZIF-8 MMMs. CO<sub>2</sub>/CH<sub>4</sub> selectivity for ZIF-67 MMMs improved more than ZIF-67 compared to pure polymer where 5 wt% ZIF-67 MMM has shown 16 selectivity and 15 wt% ZIF-8 has shown 13.76, which is 17% higher. This increase in the trend for permeability of CO<sub>2</sub> might be because of metal atom (Zn or Co) capacity for CO<sub>2</sub> adsorption, which depends on the effective metal charge and based on previous literature for various MOF of Zn and Co,<sup>44,45</sup> we can see that zinc has a higher effective metal charge which leads to higher binding strength of CO<sub>2</sub> molecule. Based on the previous statement, we can see that ZIF-8 in PES has shown higher permeability of CO<sub>2</sub> compared to ZIF-67-based MMMs. ZIF-67 MMMs have shown good CO<sub>2</sub>/CH<sub>4</sub> selectivity due to their lesser particle size compared to ZIF-8 MMMs. The increase in the CO<sub>2</sub> permeability of ZIF-8 and ZIF-67 MMMs is attributed to the CO<sub>2</sub> affinity of ZIF-MOFs and good MOF-polymer interface which can be confirmed by XRD (change in *d*-spacing) and DSC (*T<sub>g</sub>* shifting), but not due to any defect formations in the membrane which can be confirmed by Fig. 4a, b, e and f (FESEM image of MMMs).

**Comparison of *in situ* and non-*in situ* based MMMs.** Fig. S3† illustrates the comparison of mixed matrix membranes with the *in situ* method and non-*in situ* (MMMs prepared using the traditional method); a comparison is done for 1, 2, 4, and 5 wt% MMMs for both types. It can be observed that the *in situ* MMMs of ZIF-8 and ZIF-67 have outperformed traditional MMMs. For 1 wt% ZIF-8 of both non-*in situ* and *in situ* MMMs CO<sub>2</sub> permeability was 28.9 Barrer and 33.3 Barrer, respectively, *i.e.* 17% higher. 2 wt% and 4 wt% *in situ* ZIF-8 MMMs with CO<sub>2</sub> permeability enhancement of 76% (37 to 65 Barrer) and 112% (39 to 84 Barrer) respectively, 4 wt% *in situ* ZIF-8/PES MMM has shown highest CO<sub>2</sub> permeability of 84 Barrer in the overall study. 5 wt% *in situ* ZIF-8/PES MMM has shown slightly lower permeability of 61 Barrer from 41.7 Barrer (32% decrease), which can be attributed to an increase in *T<sub>g</sub>* of 227 °C, but higher than non-*in situ* 5 wt% MMM. Selectivity of CO<sub>2</sub>/CH<sub>4</sub> was also enhanced for 4 and 5 wt% *in situ* MMMs compared to non-*in situ*, which was 15.21 (from 11) and 13.97 (from 11.4), respectively, and for 1, 2 wt% ZIF-8 MMMs have CO<sub>2</sub>/CH<sub>4</sub> selectivity around was found to around pure polymeric membrane. This significant high in CO<sub>2</sub> permeability has been due to the unreacted zinc and 2-methylimidazole, which is dispersed throughout the polymer, where the CO<sub>2</sub> molecules (especially negatively charged oxygen atoms in CO<sub>2</sub>) Lewis's base interactions.<sup>46</sup>

Fig. S3(c and d)† shows the comparison study of all ZIF-67-based MMMs (*in situ* and non-*in situ*). Similar to the ZIF-8, *in situ* ZIF-67-based MMMs have shown greater CO<sub>2</sub> permeability than normal ZIF-67 MMMs due to the presence of various organic groups such as imidazole, triazine, adenine, and various others due to Lewis's acid attractions. Unlike ZIF-8, the permeability of CO<sub>2</sub> has shown an increasing trend where CO<sub>2</sub>

Table 4 *In situ* ZIF-8/PES MMMs permeation data at 0.5 bar, 1 bar, 1.5 bar

Membrane	CO <sub>2</sub> permeability (Barrer)			CO <sub>2</sub> /CH <sub>4</sub> selectivity		
	0.5 bar	1 bar	1.5 bar	0.5 bar	1 bar	1.5 bar
1 wt% <i>in situ</i> ZIF-8/PES	33.3 ± 2.43	34.3 ± 0.33	35.9 ± 0.06	11.21	12.21	10.75
2 wt% <i>in situ</i> ZIF-8/PES	65.3 ± 1.45	65.2 ± 1.21	67.5 ± 0.12	9.11	9.60	10.43
4 wt% <i>in situ</i> ZIF-8/PES	84.1 ± 1.2	84.5 ± 0.71	—	15.21	15.57	—
5 wt% <i>in situ</i> ZIF-8/PES	61.2 ± 2.46	—	—	13.97	—	—



Table 5 *In situ* ZIF-67 permeation data at 0.5 bar, 1 bar, 1.5 bar

Membrane	CO <sub>2</sub> permeability (Barrer)			CO <sub>2</sub> /CH <sub>4</sub> selectivity		
	0.5 bar	1 bar	1.5 bar	0.5 bar	1 bar	1.5 bar
1 wt% <i>in situ</i> ZIF-67/PES	27.6 ± 0.8	29.3 ± 0.21	28.6 ± 0.87	11.66	12.96	11.56
2 wt% <i>in situ</i> ZIF-67/PES	52.8 ± 0.42	54.7 ± 0.22	54.8 ± 0.35	12.76	12.83	12.18
4 wt% <i>in situ</i> ZIF-67/PES	73.7 ± 0.41	78.8 ± 0.93	—	13.47	16.39	—
5 wt% <i>in situ</i> ZIF-67/PES	79 625.6 ± 668.1	—	—	1.11	—	—

permeability was enhanced for 1, 2, 3 wt% *in situ* ZIF-67 MMMs compared to non-*in situ* ZIF-67 MMM from 22 to 27.6 Barrer, 32.9 to 52.8 Barrer and 34.8 to 73.7 Barrer, respectively. The 5 wt% *in situ* ZIF-67/PES MMM has shown an exponential increase of CO<sub>2</sub> permeability of 79 625 Barrer formation of defects (FESEM image, Fig. 4h) which occurred due to the growth of ZIF-67 in PES. CO<sub>2</sub>/CH<sub>4</sub> selectivity of *in situ* ZIF-67/ MMMs has enhanced similarly to all previously reported literature<sup>47</sup> The enhancement of CO<sub>2</sub> permeability is attributed to the pore walls of ZIF-67 being slightly electropositive, which is implied due to the availability of Co<sup>2+</sup> sites as discussed

previously, have electronegativity, which provides various transport channels for CO<sub>2</sub> transport.

**Comparison with existing literature.** Table 6 provides the literature data on various membrane – preparation technique and their gas permeation results some studies are discussed in the introduction section. S. Park *et al.*<sup>18</sup> have studied the effect of *in situ* coating by coating PAA on  $\alpha$ -alumina supports, followed by immersion in zinc and benzimidazole linker solutions to form ZIF-7 on top of the PAA layer. This was followed by thermal imidization, which resulted in a slight decrease in CO<sub>2</sub> permeability from 433 to 74 Barrer, but an increase in selectivity

Table 6 Comparison of permeation data with existing literature

Membrane	Preparation technique (FS-flat sheet, HF-hollow fiber)	Testing pressure (bar)	Feed type (P-pure/single gas, M-mixed gas)	Permeability, Selectivity	Reference	
				$P_{CO_2}$ (Barrer)	$\alpha_{CO_2/CH_4}$	
ZIF-7/PAA	ZIF-7 preparation on PI coated on $\alpha$ -alumina (FS)	1	P	74	36	18
NH <sub>2</sub> -ZIF-8/PVAm/mPSF	<i>In situ</i> grafting of PeA on ZIF-8 and coated on PVAm/mPSF (FS)	10	P	3800 GPU	50	20
ZIF-8/Pebax	One pot synthesis of ZIF-8 in Pebax polymer (FS)	10	P	158	25	23
ZIF-8/PSF	The traditional way of mixed matrix membrane (FS)	0.5	M	25	12	34
NH <sub>2</sub> ZIF-8/PSF	The traditional way of mixed matrix membrane (FS)	0.5	M	21	14	34
ZIF-8/CA	The traditional way of mixed matrix membrane (FS)	0.5	M	9.5	15.3	40
ZIF-8/Pebax	The traditional way of mixed matrix membrane (FS)	11	P	130	18.6	47
ZIF-67/Pebax	The traditional way of mixed matrix membrane (FS)	11	P	162	25	47
ZIF-8/PES	Dip coating of ZIF-8 on porous PES membrane (FS)	2	M	22 GPU	14.6	48
ZIF-8/PEI	The traditional way of mixed matrix membrane (FS)	1	M	0.8	12.5	49
ZIF-67/PEI	The traditional way of mixed matrix membrane (FS)	1	M	0.5	10.4	49
ZIF-67/PSF-GO	<i>In situ</i> growth of ZIF-67 on PSF/GO (HF)	1	M	39.3 GPU	44.9	50
ZIF-8/PSF	The traditional way of mixed matrix membrane (FS)	4	P	29.22	23.16	51
ZIF-8/PES	The traditional way of mixed matrix membrane (FS)	1.5	M	75.6	13.8	Present work
ZIF-67/PES	The traditional way of mixed matrix membrane (FS)	1.5	M	68	14.6	Present work
<i>In situ</i> ZIF-8/PES	<i>In situ</i> synthesis of ZIF-8 in PES (FS)	2	M	84.5	15.6	Present work
<i>In situ</i> ZIF-67/PES	<i>In situ</i> synthesis of ZIF-67 in PES (FS)	2	M	78.8	16.4	Present work



of  $\text{CO}_2/\text{CH}_4$  from 29 to 36. In another *in situ* investigation, polyethylene amine (PeA) grafted *in situ* on ZIF-8, dispersed in poly (vinyl amine) (PVAm), coated with modified polysulfone (mPSF) substrate. This resulted in an increase in  $\text{CO}_2/\text{CH}_4$  selectivity from 20 to 50 and an increase in  $\text{CO}_2$  permeance of about 3800 GPU.<sup>20</sup> Maleh and Raisi<sup>23</sup> have performed *in situ* techniques to synthesize ZIF-8 MOF in Pebax polymer *via* one-pot synthesis and coated on a PES layer. At 8 bar feed pressure, the permeability of  $\text{CO}_2$  and  $\text{CO}_2/\text{CH}_4$  selectivity was found to be 158 Barrer and 25, respectively, surpassing the Robeson lower bound. Mixed matrix membranes were prepared by dispersing ZIF-8 and ZIF-67 in Pebax MH-1657 polymer *via* solvent evaporation technique and at higher filler loading (20 wt%) to check the compatibility with polymer and gas separation performance of both fillers. ZIF-8 and ZIF-67 MMMs  $\text{CO}_2$  permeability was 130 and 162 and  $\text{CO}_2/\text{CH}_4$  selectivity was 18.6 and 25 higher than polymer.<sup>47</sup> These results show the superior performance of ZIF-67 over ZIF-8, due to the electrostatic interaction of Zn-metal in ZIF-8 with  $\text{CO}_2$ , limiting its diffusion through the membrane, which is corroborated by solubility and diffusion results. Thin ZIF-8 membranes were fabricated on PES-ZIF-8 (MMM support) *via* *in situ* secondary growth; prepared membranes showed the same  $\text{CO}_2$  permeability as pure polymer, whereas  $\text{CO}_2/\text{CH}_4$  selectivity was enhanced from 9 to 14.6.<sup>48</sup> This improvement of selectivity in *in situ* (ZIF-8/PES) membranes shows the molecular sieving capability of ZIF-8 MOF and also shows good interaction between ZIF-8 and PES polymeric support from FESEM results. Polyetherimide-based MMMs were fabricated using ZIF-8 and ZIF-67 and at 10 wt% filler loading  $\text{CO}_2$  permeability was 0.6 (ZIF-8/PEI) and 0.5 Barrer (ZIF-67/PEI), and  $\text{CO}_2/\text{CH}_4$  selectivity of 12.5 and 10.4 for ZIF-8/PEI and ZIF-67/PEI MMM respectively.<sup>49</sup> This study provides in-sights to the limitations of polyetherimide polymer-based membranes for gas separation which can be surpassed by the addition of ZIF-based fillers. *In situ* growth of ZIF-67 MOF was done on PSF/GO hollow fibers, and  $\text{CO}_2$  permeability of 39.3 GPU (slightly less than polymer) and selectivity of  $\text{CO}_2/\text{CH}_4$  was 45, almost doubled from pure polymer.<sup>50</sup> This increase in the  $\text{CO}_2$  permeation was due to oxygen-rich functional groups on the surface of GO-sheets and the tortuous path provided by the filler. Asymmetric PSF-based mixed matrix membranes were fabricated at lower filler loading of ZIF-8 for  $\text{CO}_2/\text{CH}_4$  separation and tested with pure gases at 4 bar pressure, at 0.5 wt% ZIF-8  $\text{CO}_2$  permeability obtained 29.22 GPU and  $\text{CO}_2/\text{CH}_4$  selectivity was increased to 23.16,<sup>51</sup> improvement in the gas permeability is attributed to the settling of ZIF-8 particles in the pores of PSF polymer while preparation of membrane which is observed in its FESEM images. In the present work, we can see that the permeability of  $\text{CO}_2$  has surpassed some of the previous literature<sup>18,34,48,49</sup> while attaining the  $\text{CO}_2/\text{CH}_4$  selectivity for both *in situ* and non-*in situ*, whereas few literature MMMs studies either permeability or selectivity has decreased compared to pure polymeric membrane.<sup>40</sup>

Compared to the literature, we can see that filler-induced (especially ZIF-8 and ZIF-67) and *in situ* mixed matrix membranes have shown superior performance for the separation of  $\text{CO}_2$  compared to pure polymeric membranes. In

summary, various *in situ* strategies (even other MOFs) for the fabrication of MMMs have more effective ways to improve their performance.

## 4 Conclusion

This paper demonstrated the preparation and characterization of *in situ* ZIF-8, and ZIF-67 MMMs and their significance in  $\text{CO}_2/\text{CH}_4$  separation *via* gas permeation experiments. The membranes were characterized using FTIR for conformation of ZIF-8 and ZIF-67 in membranes and FESEM for the difference in particle size of ZIF-8 and ZIF-67 in different filler loadings and *in situ* preparation. DSC was done in membranes to find changes in glass transition temperature ( $T_g$ ). The properties of traditional and *in situ* MMMs can be seen *via* FESEM and DSC results, where different morphology for *in situ* grown ZIF-8 and ZIF-67 MOFs compared to normal MOF particles was observed and also, we can see different thermal properties of traditional and *in situ* MMMs *via* shift in  $T_g$  values. Fabricated MMMs performance was assessed with mixed gas (40%- $\text{CO}_2$  and 60%- $\text{CH}_4$ ) as feed at three different pressure differences 0.5, 1, and 1.5 bar. The  $\text{CO}_2$  permeability of *in situ* ZIF-8 and *in situ* ZIF-67-based MMMs was enhanced to 84.1 Barrer (250% increase) for 4 wt% *in situ* ZIF-8/PES MMM and 73.7 Barrer (207% increase) for 4 wt% *in situ* ZIF-67/PES from 24 Barrer (pure PES membrane). Similar increases in permeability of  $\text{CO}_2$  were seen in the ZIF-8 and ZIF-67 based MMMs, 75.6 Barrer for 15 wt% ZIF-8/PES and 68 Barrer for 15 wt% ZIF-67/PES. Also, due to the molecular sieving effect, the highest selectivity of 16.4 was observed for 4 wt% *in situ* ZIF-67/PES at a 1 bar pressure difference. A detailed comparison was given for ZIF-8 vs. ZIF-67 MMMs, *in situ* ZIF-8 vs. *in situ* ZIF-67 MMMs, and *in situ* vs. non-*in situ* membranes. Fabricated ZIF-8 and ZIF-67 *in situ* membranes have good scope in the upgradation of biogas to Bio-CNG, due to their higher  $\text{CO}_2/\text{CH}_4$  separation performance.

## Data availability

The authors declare that the data supporting the findings of this study are available within the paper.

## Author contributions

Aditya Jonnalagedda (AJ): conceptualization, methodology, investigation, data curation, writing-original draft; Bhanu Vardhan Reddy Kuncharam (BVRK): conceptualization, methodology, formal analysis, visualization, writing-review & editing, funding acquisition, supervision.

## Conflicts of interest

The authors have no relevant financial or non-financial interests to disclose.



## References

1 K. S. Demirchian and K. K. Demirchian, *Energy Convers. Manage.*, 1996, **37**, 1265–1270.

2 C. Bonechi, M. Consumi, A. Donati, G. Leone, A. Magnani, G. Tamasi and C. Rossi, in *Bioenergy Systems for the Future*, Elsevier, 2017, pp. 3–42.

3 O. W. Awe, Y. Zhao, A. Nzihou, D. P. Minh and N. Lyczko, *Waste Biomass Valorization*, 2017, **8**, 267–283.

4 X. Y. Chen, H. Vinh-Thang, A. A. Ramirez, D. Rodrigue and S. Kaliaguine, *RSC Adv.*, 2015, **5**, 24399–24448.

5 N. Nady, N. Salem and S. H. Kandil, *Sci. Rep.*, 2022, **12**, 13675.

6 R. L. Burns and W. J. Koros, *J. Membr. Sci.*, 2003, **211**, 299–309.

7 P. S. Goh, A. F. Ismail, S. M. Sanip, B. C. Ng and M. Aziz, *Sep. Purif. Technol.*, 2011, **81**, 243–264.

8 L. M. Robeson, *J. Membr. Sci.*, 1991, **62**, 165–185.

9 L. M. Robeson, *J. Membr. Sci.*, 2008, **320**, 390–400.

10 P. Tanvidkar, S. Appari and B. V. R. Kuncharam, *Rev. Environ. Sci. Biotechnol.*, 2022, **21**, 539–569.

11 M. R. Abdul Hamid, Y. Qian, R. Wei, Z. Li, Y. Pan, Z. Lai and H.-K. Jeong, *J. Membr. Sci.*, 2021, **640**, 119802.

12 L. Zhang, L. Feng, P. Li, X. Chen, J. Jiang, S. Zhang, C. Zhang, A. Zhang, G. Chen and H. Wang, *Chem. Eng. J.*, 2020, **395**, 125072.

13 X. Zhu, H. Zhao, H. Wang, D. Yang, F. Liu and X. Song, *J. Polym. Environ.*, 2024, **32**, 2884–2896.

14 D. Matatagui, A. Sainz-Vidal, I. Gràcia, E. Figueras, C. Cané and J. M. Saniger, *Sens. Actuators, B*, 2018, **274**, 601–608.

15 H. Kaur, G. C. Mohanta, V. Gupta, D. Kukkar and S. Tyagi, *J. Drug Delivery Sci. Technol.*, 2017, **41**, 106–112.

16 R. Banerjee, A. Phan, B. Wang, C. Knobler, H. Furukawa, M. O'Keeffe and O. M. Yaghi, *Science*, 2008, **319**, 939–943.

17 Y. Jia, P. Liu, Y. Liu, D. Zhang, Y. Ning, C. Xu and Y. Zhang, *Fuel*, 2023, **339**, 126938.

18 S. Park, K. Y. Cho and H.-K. Jeong, *J. Mater. Chem. A*, 2020, **8**, 11210–11217.

19 S. Park, M. R. Abdul Hamid and H. K. Jeong, *ACS Appl. Mater. Interfaces*, 2019, **11**, 25949–25957.

20 Y. Gao, Z. Qiao, S. Zhao, Z. Wang and J. Wang, *J. Mater. Chem. A*, 2018, **6**, 3151–3161.

21 X. Li, S. Yu, K. Li, C. Ma, J. Zhang, H. Li, X. Chang, L. Zhu and Q. Xue, *Sep. Purif. Technol.*, 2020, **248**, 117080.

22 A. M. Marti, S. R. Venna, E. A. Roth, J. T. Culp and D. P. Hopkinson, *ACS Appl. Mater. Interfaces*, 2018, **10**, 24784–24790.

23 M. S. Maleh and A. Raisi, *Chem. Eng. Res. Des.*, 2022, **186**, 266–275.

24 H. R. Amedi and M. Aghajani, *Microporous Mesoporous Mater.*, 2017, **247**, 124–135.

25 X. Guo, T. Xing, Y. Lou and J. Chen, *J. Solid State Chem.*, 2016, **235**, 107–112.

26 P. Tanvidkar, A. Jonnalagedda and B. V. R. Kuncharam, *J. Appl. Polym. Sci.*, 2023, **140**, e53264.

27 Y. Pan, Y. Liu, G. Zeng, L. Zhao and Z. Lai, *Chem. Commun.*, 2011, **47**, 2071–2073.

28 A. Schejn, L. Balan, V. Falk, L. Aranda, G. Medjahdi and R. Schneider, *CrystEngComm*, 2014, **16**, 4493–4500.

29 C.-Y. Liang, P. Uchytíl, R. Petrychkovych, Y.-C. Lai, K. Friess, M. Sipek, M. Mohan Reddy and S.-Y. Suen, *Sep. Purif. Technol.*, 2012, **92**, 57–63.

30 B. Nayak, P. Tanvidkar and B. V. R. Kuncharam, *Polym. Eng. Sci.*, 2023, **64**, 788–797.

31 Y. Hu, H. Kazemian, S. Rohani, Y. Huang and Y. Song, *Chem. Commun.*, 2011, **47**, 12694–12696.

32 H. Abdul Mannan, H. Mukhtar, M. Shima Shaharun, M. Roslee Othman and T. Murugesan, *J. Appl. Polym. Sci.*, 2016, **133**(5), 42946.

33 H. Y. Hwang, D. J. Kim, W. J. Yim and S. Y. Nam, *Desalination*, 2012, **289**, 72–80.

34 A. Jonnalagedda and B. V. R. Kuncharam, *J. Appl. Polym. Sci.*, 2023, **140**(45), e54650.

35 P. Y. Moh, M. Brenda, M. W. Anderson and M. P. Attfield, *CrystEngComm*, 2013, **15**, 9672–9678.

36 B. Seoane, J. M. Zamaro, C. Tellez and J. Coronas, *CrystEngComm*, 2012, **14**, 3103.

37 M. J. Van Vleet, T. Weng, X. Li and J. R. Schmidt, *Chem. Rev.*, 2018, **118**, 3681–3721.

38 P. Choudhary, N. Saini, M. H. Yoon, K. Awasthi and K. Pandey, *Environ. Sci. Pollut. Res.*, 2023, **30**, 105387–105397.

39 M. Z. Ahmad, V. Martin-Gil, V. Perfilov, P. Sysel and V. Fila, *Sep. Purif. Technol.*, 2018, **207**, 523–534.

40 P. Tanvidkar, A. Jonnalagedda and B. V. R. Kuncharam, *Environ. Technol.*, 2023, **45**(14), 2867–2878.

41 M. S. Maleh and A. Raisi, *Colloids Surf. A*, 2023, **659**, 130747.

42 N. Missaoui, A. Chrouda, H. Kahri, A. J. Gross, M. Rezaei Ardani, A. L. Pang and M. Ahmadipour, *Sep. Purif. Technol.*, 2023, **316**, 123755.

43 M. B. K. Niazi, Z. Jahan, A. Ahmed, S. Rafiq, F. Jamil and Ø. W. Gregersen, *J. Polym. Environ.*, 2020, **28**, 1921–1933.

44 D. Yu, A. O. Yazaydin, J. R. Lane, P. D. C. Dietzel and R. Q. Snurr, *Chem. Sci.*, 2013, **4**, 3544.

45 H. S. Koh, M. K. Rana, J. Hwang and D. J. Siegel, *Phys. Chem. Chem. Phys.*, 2013, **15**, 4573.

46 Y. Dai, X. Ruan, Z. Yan, K. Yang, M. Yu, H. Li, W. Zhao and G. He, *Sep. Purif. Technol.*, 2016, **166**, 171–180.

47 S. Meshkat, S. Kaliaguine and D. Rodrigue, *Sep. Purif. Technol.*, 2020, **235**, 116150.

48 Z. Y. Yeo, P. Y. Tan, S.-P. Chai, P. W. Zhu and A. R. Mohamed, *RSC Adv.*, 2014, **4**, 52461–52466.

49 J. Vega, A. Andrio, A. A. Lemus, J. A. I. Díaz, L. F. del Castillo, R. Gavara and V. Compañ, *Sep. Purif. Technol.*, 2019, **212**, 474–482.

50 K. Sainath, A. Modi and J. Bellare, *J. Membr. Sci.*, 2020, **614**, 118506.

51 N. A. H. Md. Nordin, A. F. Ismail, A. Mustafa, R. S. Murali and T. Matsuura, *RSC Adv.*, 2015, **5**, 30206–30215.

